Post-print version of the article published in Desalination:
M. Micari, M. Moser, A. Cipollina, A. Tamburini, G. Micale, V. Bertsch
Towards the Implementation of Circular Economy in the Water Softening Industry: A Technical, Economic and Environmental Analysis, Journal of Cleaner Production, 255, 2020, 120291. https://doi.org/10.1016/j.jclepro.2020.120291

TOWARDS THE IMPLEMENTATION OF CIRCULAR ECONOMY IN THE WATER SOFTENING INDUSTRY: A TECHNICAL, ECONOMIC AND ENVIRONMENTAL ANALYSIS

M. Micari[1]*, M. Moser[1], A. Cipollina[2], A. Tamburini[2]*, G. Micale[2], V. Bertsch[1,3]

1 German Aerospace Center (DLR), Institute of Engineering Thermodynamics, Pfaffenwaldring 38-40, 70569 Stuttgart, Germany

2 Dipartimento di Ingegneria, Università degli Studi di Palermo (UNIPA), viale delle Scienze Ed. 6, 90128 Palermo, Italy

3 University of Stuttgart, Institute for Building Energetics, Thermotechnology and Energy Storage, Pfaffenwaldring 6, 70569 Stuttgart, Germany

*corresponding authors: alessandro.tamburini@unipa.it; Marina.micari@dlr.de

ABSTRACT

The implementation of a circular economy approach at the industrial level is typically performed via the introduction of cleaner production strategies. This work aims at the identification of the most suitable strategy to improve the sustainability of the water softening industry via the treatment and recycling of the produced wastewater. For the first time, different concentration technologies and different energy supply systems are compared to minimize the environmental impact of the industrial process and to ensure the economic feasibility of the treatment system. The comparison concerns three treatment chains, each one composed of the same pre-treatment step and different concentration technologies: Multi-Effect Distillation (MED), Membrane Distillation (MD) and the coupling of Reverse Osmosis and Membrane Distillation (RO-MD). Firstly, the effect of different feed flow rates and thermal energy costs is investigated. Secondly, the impact of different drivers, as the electricity self-generation via a PhotoVoltaic-battery plant and the meteorological characteristics of the plant location, is analysed. Results indicate that the MED-chain is the most feasible at higher plant sizes, thanks to its lower energy demand, while the one including RO-MD shows lower costs at smaller plant sizes, because of its lower investment costs. The

MD-chain turns out to be the worst performing in all cases. When a renewable energy source is coupled, both the MED-chain and RO-MD-chain show a net reduction of the carbon dioxide emissions with respect to the ones produced by the current technology. Furthermore, their global costs are very competitive, especially if the plant is located in a region with high solar potential.

KEYWORDS

Industrial Wastewater, Circular Economy, Treatment chain, CO_2 emissions, Recycling, Membrane Processes

1. INTRODUCTION

Sustainable development is considered the only feasible answer to the simultaneous growth of energy and water demand and the increase in environmental pollution. According to the definition given by the Brundtland commission in 1987, sustainable development is able to "*meet the needs of the present without compromising the ability of future generations to meet their own needs*" [1]. Beside energy savings and large-scale introduction of renewable energies, one of the most acknowledged ways to achieve a more sustainable development consists in the application of the circular economy concept. The concept was originally introduced by Boulding in 1966 and is based on the fact that the economy has to be a circular system to ensure the sustainability of human life on Earth [2]. According to the widely accepted definition given by the Ellen MacArthur Foundation, circular economy is "*an industrial economy that is restorative and regenerative by intention and design*" [3]. The main objective of circular economy is the promotion of a more appropriate and environmentally friendly management of resources, to implement a greener economy [4]. Circular economy takes into consideration social, technological and economic aspects of the investigated industrial process or sector and their mutual interactions and proposes new business models and technological solutions, which may radically change the traditional patterns and introduce new, more sustainable ones [5], [11]. This often requires a complete redesign of the industrial processes, which promotes the industry-environment interactions and the bi-directional flows of material and energy [6]. In other words, circular economy aims at a closed loop of material flows which does not have net effects on the environment, in contrast to a linear economy approach where the natural resources are converted into waste via production, leading to a continuous deterioration of the environment [7], [8]. This

approach allows achieving a *cleaner* industrial production, which leads to pollution prevention, reduction of the employment of toxic substances and decrease of damage and risks for humans and for the environment [9], [10]. For this scope, the choice of the technologies to implement should be made taking into account different indicators, such as CO_2 emissions, water and energy requirements, costs, labour conditions, economic growth, and how these aspects are interrelated [11].

A number of works in literature are focused on the implementation of circular economy at the industrial level, investigating new strategies to treat the waste streams with the aim to produce (i) sellable raw materials and/or (ii) material streams to be reused in the industrial process. Significant attention has been devoted to the food industry sector, where the production of waste occurs during all the food life cycle, from the agriculture to the manufacturing and consumption phases [12]. Depending on the specific food, different types of waste are produced and consequently different substances may be extracted [13], [14]. Sugar industry produces a significant amount of various waste materials and several possible waste valorisation strategies have been proposed in literature, such as the employment of the sugarcane biomass for energy production [15], [16]. Textile industry is another sector in which the production of wastewater streams represents a severe issue. The most contaminated stream is the dyeing discharge, which may have a severe negative impact on the environment, because it contains a high amount of colour and organic compounds, together with salt [17]. Therefore, many studies focused on the development of new treatment strategies, including decolourization and oxidation processes, with the aim to recycle the treated effluent as fresh dyeing solution [18], [19]. Finally, other industrial sectors are characterized by very high water consumption and, as a consequence, by the production of significant volumes of wastewaters, such as paper, laundering and coal mine industry. To achieve a sustainable production, the wastewater may be treated to reduce the organics content [20] and to recover valuable materials, such as water and detergent in the laundering industry [21] and salts as well as rare earth elements in the coal mine industry [22], [23].

The aim of this work is to identify the most suitable treatment chains to achieve a *cleaner* production in the industrial process of water softening, performed via ion exchange resins. The plant taken as a reference in the present work is owned by the water industry Evides and it is located in Rotterdam, The Netherlands. Water softening is a water purification process, which aims at removing the hardness (Magnesium and Calcium ions) from the water. Periodically, the resins have to be regenerated with a NaCl-water solution and the regeneration produces a wastewater stream, containing a high amount of sodium and chloride

ions, together with bivalent ions (Magnesium, Calcium and Sulphate ions). Currently, this effluent is disposed into the sea, since there are no organic pollutants or harmful components. However, the concentration of the bivalent ions is much higher than in seawater and large volumes of effluent are produced. In addition, the treatment of the effluent could lead to a net reduction of the demand of reactants for the IEX regeneration process itself. Therefore, to reduce the demand of raw materials and to limit the environmental pollution due to the effluent disposal, we devised a suitable treatment chain, presenting pre-treatment and concentration steps. The pre-treatment processes aim at separating the bivalent ions, while in the concentration steps the remaining NaCl-water solution is concentrated up to the concentration of the fresh regenerant solution to be reused in the industrial process for the following regeneration cycle. More precisely, the pre-treatment step presents the combination of nanofiltration and crystallization, while three alternative technologies are considered for the concentration step: (i) multi-effect distillation (MED), (ii) membrane distillation (MD) and (iii) reverse osmosis coupled with membrane distillation (RO-MD). A schematic representation of the treatment chains investigated in the present work is reported in Figure 1. The case study has been already introduced by the same authors in two previous works, whose aims were (i) to optimize the multi-effect distillation for this specific application [47] and (ii) to assess the influence of the operating conditions of the nanofiltration on the global figures of the chain [28], respectively.

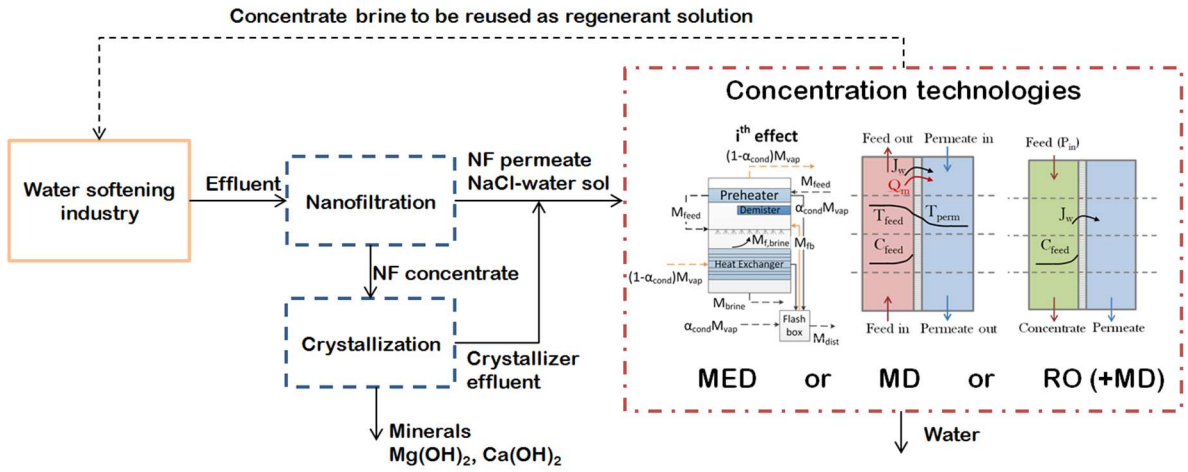

Figure 1. Schematic representation of the treatment chains for the presented case study. The industrial process is represented by the box framed in yellow (solid line), the pre-treatment steps by the ones in blue (dashed line) and the concentration step alternatives in red (dash-dotted line).

This work presents a comprehensive analysis of the concentration processes that may be performed to treat and recycle the wastewater coming from the water softening industry and,

for the first time, different technologies and different energy sources are compared to find the most economically feasible and environmentally friendly treatment system. Firstly, this work aims at identifying the best performing technology or combination of technologies to be implemented in the concentration step, via the assessment of the economic feasibility, the energy requirements and the environmental impact due to the CO_2 emissions. Secondly, we investigate the impact of different drivers on the selected technologies, with a focus on the self-generation of electricity via a PV-battery plant and on the meteorological and geographical conditions of the region selected for the plant location.

Overall, for the first time, a comprehensive study, including different concentration technologies and renewable energy supply systems, is presented to investigate the potential of the implementation of a circular economy approach in the water softening industry.

2. MATERIALS AND METHODS

The treatment chains presented in Figure 1 are given by the combination of different processes. We implemented techno-economic models to simulate each unit and then, we interconnected the units to reproduce the behaviour of the whole system. In the following, a short description of the techno-economic models is reported, while the models relevant to NF and MED were described in more details in previous works [28], [47] and the ones relevant to RO and MD are presented in the Supplementary Materials. In the second paragraph, the parameters used for the comparison of the chains are defined and the scenarios including different energy supply systems are described.

2.1 Techno-economic models

Nanofiltration.

Nanofiltration is a pressure-driven membrane process, in which the purification of the feed solution is realized via the employment of a porous membrane. Three different exclusion mechanisms occur at the feed-membrane interface, i.e. size exclusion, based on the steric effect; Donnan exclusion, based on the potential gradient at the interface; and dielectric exclusion, based on the different dielectric constant between bulk and pores. This leads to a very high membrane rejection to the bivalent and multivalent ions, which is the main reason why the NF unit is employed as a pre-treatment step.

We implemented a multi-scale model including three different scales. For the membrane model (*low-hierarchy model*), one of the most popular modelling approaches, the Donnan

Steric Pore Model with Dielectric Exclusion (DSPM-DE), was implemented. The model provides the resolution of the extended Nernst-Plank equation within the thickness of the membrane and takes into account the boundary conditions given by the exclusion mechanisms [24–26]. The main results of the low-scale model consist in the rejection for every ion and the water flux J_v. These are some of the inputs of the *medium-hierarchy model*, which describes the NF unit along the feed main flow direction. Thus, mass balances are applied to define the concentration and flow rate on the permeate and the feed side for each discretization step [27]. Finally, the *high-hierarchy model* estimates the required size of the NF plant, given by NF units arranged in series and in parallel, to achieve a certain total recovery (defined as the ratio between permeate and feed flow rate). Regarding the energy demand, the NF process requires electricity to pump the feed up to the defined pressure. The economic model follows the Verberne cost model [44]. The operating conditions of the NF plant are the ones which we previously found to be the most economically competitive, i.e. feed pressure of 20bar and recovery of 25% [28]. The employed membrane rejections are equal to 94.8% for Mg^{++}, 83% for Ca^{++}, 93.6% for $SO4^{--}$, -50.6% for Na^{+} and 49.9% for Cl^{-}, which are in line with values reported in literature [29].

Crystallization.

Crystallization is a key unit in the chains, since its products, mainly $Mg(OH)_2$, are highly valuable materials, whose production strongly contributes to the economic feasibility of the chain. $Mg(OH)_2$ and $Ca(OH)_2$ are supposed to be produced separately in two following crystallizers, which make use of a NaOH-water solution as alkaline reactant. Each crystallizer is followed by a filter, where the crystals are obtained from the magma produced in the crystallizer. For this process, we implemented a simplified model based on mass balances under the assumption of a 100% conversion of the dissolved Mg^{++} and Ca^{++} into $Mg(OH)_2$ and $Ca(OH)_2$ respectively [30]. Mass balances are employed to estimate the total amount of produced crystals, the outlet effluent concentration and flow rate and the required amount of reactants. For what concerns the energy demand of the crystallization step, two terms are estimated: (i) the pumping energy to pump the solutions to the crystallizers and (ii) the electric energy required by the filters. Finally, for the estimation of the capital costs, the Module Costing Technique is applied, with suitable parameters for crystallizers and filters found in literature [31].

Multi-Effect Distillation.

The MED process has been widely investigated in literature, mostly for seawater desalination purposes [32–34]. The MED model implemented for this work presents a forward-feed arrangement, since it is more suitable to the high temperatures and concentrations which are expected to be reached in the investigated cases. The plant is composed of a certain number of stages in series, each one presenting a heat exchanger, where partial evaporation of the feed occurs, and a preheater, where the feed is heated up before entering inside the stage. The number of stages is fixed and equal to 13, as it resulted to be the optimum value from a previous MED cost minimization analysis [47]. The thermal energy is supplied to the first effect in the form of vapour at a pressure of 1bar. Finally, the distillate produced is supposed to be pure water and the concentration of the brine is a constraint. The model includes an iterative procedure, which runs until the three following conditions are simultaneously achieved: (i) the areas of the heat exchangers at each stage are equal, (ii) the areas of the preheaters are equal and (iii) the outlet distillate flow rate fulfils the overall mass balances, depending on the required brine concentration.

As concerns the energy requirements, the thermal energy is the prominent term, given by the required amount of steam multiplied by the latent heat at the pressure of 1bar. The electricity demand is fixed and equal to 1.5kWh/m^3_{dist} [35]. The details of the economic model are reported in a previous work [47].

Reverse Osmosis.

Reverse Osmosis is a very common desalination process, based on a membrane separation under an applied pressure. The model has a hierarchical structure, as shown in more detail in the Supplementary Materials: it goes from the investigation of the membrane properties and the estimation of the fluxes to the design of a whole plant. The RO plant typically presents many vessels arranged in parallel to reach a certain total recovery, similarly to the NF plant [36]. Each vessel contains a number of RO units in series, each with spiral-wound geometry. For what concerns the energy demand, RO requires only electricity to pump the feed up to the inlet pressure. Finally, the economic model includes the calculation of the capital costs, composed of the costs of the membrane elements, pressure vessels, high pressure pumps, piping and intake costs [37], [38], [42]. Among the operating costs, the one due to the electric energy demand constitutes the most significant term. The other operating costs concern maintenance (3%/y of the investment plus 20% of the annual labour cost), labour, chemicals and membrane replacement [42].

Membrane Distillation.

MD is a separation process, which makes use of a microporous hydrophobic membrane, permeable only to water vapour. The driving force consists in the vapour pressure difference at the two membrane interfaces, due to a temperature difference, which generates a vapour flux through the membrane. The model implemented for this work describes a Direct Contact MD (DCMD) configuration, which was selected for its simplicity and for the high vapour fluxes [39]. The details of the implemented model are reported in Supplementary Materials. In the *DCMD membrane model*, the heat and mass transfer phenomena are investigated to define the vapour flux through the membrane. In the *DCMD unit model*, mass and energy balances are set up to investigate the flow rate, concentration and temperature profiles along the feed stream-wise direction. Finally, the *DCMD plant model* is able to simulate a high-scale plant, where the MD units are arranged in series and in parallel to reach a high recovery. Regarding the energy consumption, thermal energy is required to increase the temperature of the feed from the intake temperature to the inlet temperature (usually 80°C) and in each intermediate heater. Electric energy is required to pump the feed and the permeate entering each module in series. The economic model includes the capital costs, given by the costs of modules, membrane, pumps and heat exchangers, together with the cost for intake and pre-treatment. Conversely, the operating costs comprise the electric and thermal energy demand, maintenance (2.5%/y of the investment cost without the cost of membranes and modules), labour, chemicals and membrane replacement cost [41], [43].

2.2 Global outputs of the treatment chains and energy supply

Global outputs

To be able to properly compare the treatment chains, we defined some representative output values, which are relevant to the technical, economic and environmental performances of the whole system. Concerning the technical aspects, the thermal and electric energy demands [kW] have been adopted as the reference outputs to compare the different technologies. Concerning the economic analysis, the capital costs are estimated for each process and annualized using a fixed discount rate and a life time, which is specific to the unit. The operating costs depend on several parameters, such as pumps efficiency, capacity factor of the plant and cost of utilities. Finally, the revenues are proportional to the selling prices of the by-products. The most significant parameters are summarized in Table 1. Overall, for each unit it is possible to calculate the relevant CAPEX and OPEX in [$/y]. In order to summarize all the terms of cost of a treatment chain, a global levelized cost is used, which represents the selling

price that the main product of the chain would have at the break-even point and which takes into account all the capital and operating expenses of the units and the revenues coming from the other by-products. In the present case, the main product is the concentrate brine which can be reused as a reactant solution in the industrial process and a global parameter called Levelized Brine Cost (LBC [$/m$^3_{brine}$]) is taken as the reference economic output [47].

$$\mathrm{LBC_{tot}} = \mathrm{LBC_{cap}} + \mathrm{LBC_{op}} = \frac{\sum_{units} \mathrm{CAPEX}}{\mathrm{Q_{brine}}} + \frac{\sum_{units} \mathrm{OPEX} - \mathrm{Revenue_{Mg(OH)_2}} - \mathrm{Revenue_{Ca(OH)_2}} - \mathrm{Revenue_{water}}}{\mathrm{Q_{brine}}} \quad (1)$$

Table 1. Parameters used for the economic analyses.

Parameter	Value	Units
Discount rate	6	%
Units' life time (Straight line depreciation)	• NF, structure: 30 [44] • NF, electrical and mechanical: 15 [44] • Crystallizer: 20 • RO: 25 [42] • MED: 25 [40] • MD: 10 [41]	y
Capacity factor	0.94	-
Pumps' efficiency	0.8	-
Cost of electricity	0.103	$/kWh
Cost of thermal energy	0.01	$/kWh
Replacement rate of membranes	RO, MD: 15 [42], [43] NF: 20 [44]	%/y
Price of $Mg(OH)_2$	1200 [45]	$/ton
Price of $Ca(OH)_2$	300 [45]	$/ton
Price/cost of water	1 [46]	$/m3
Cost of NaCl for the regenerant solution (current technology)	80 [47]	$/ton

Finally, regarding the environmental aspects, the attention is focused only on the CO_2 emissions [kt/y] or [kg/m$^3_{prod}$] due to the thermal and electric energy supply. In particular, the CO_2 emissions per m^3 of produced regenerant solution are considered to compare the proposed treatment chains with the current system. In analogy with the economic feasibility, the sustainability enhancement is evaluated by comparing the emissions of the treatment

chains per m^3 of produced brine with the current emissions due to the production of the regenerant solution.

Energy supply

The energy supply plays a significant role in the analyses performed in the present work, as it strongly influences the operating costs and the environmental impact of the process. For this reason, the role of the electricity supply is assessed analysing *two scenarios*:

1. in the first, the electricity is completely taken from the grid;
2. in the second, the electricity is mostly supplied by a photovoltaic power plant, with Li-Ion battery storage units operating in conjunction, while the remaining fraction of required electricity is taken from the grid. The photovoltaic technology has been chosen rather than the wind technology, because it is more modular and easier to handle and because it is more regular in the power production. The natural irregularity of the wind makes necessary to implement oversized batteries, which would lead to much higher LCOE values.

Regarding the *first scenario*, the current mix of electricity carriers of the grid relevant to the specific country (The Netherlands) is considered, with the corresponding efficiencies and CO_2 emission factors, reported in Table 2. The combination of the emission factors of the single carriers, their efficiency and share of the electricity output give rise to a global CO_2 grid intensity equal to $0.471 kg_{CO2}/kWh$.

Table 2. Electricity carriers' mix in the grid in The Netherlands in 2016: electricity output, efficiency and CO_2 emission factor for each carrier [48], [49].

Electricity Carriers The Netherland (2016)	**Electricity output [TWh]**	**Electricity output [%]**	**Efficiency (total output) [-]**	**CO_2 emission factor [kg/kWh$_{prim\ energy}$]**
Hard Coal, coal products	41.5	37.69	0.42	0.335
Natural Gas	49.4	44.87	0.54	0.201
Biomass	4.9	4.45	0.34	-
Mineral oil product	1.4	1.27	1	0.27
Nuclear	4.1	3.72	0.33	-
Hydro	0.1	0.09	1	-
PV	1.1	1.00	1	-
Wind	7.6	6.90	1	-
Total	110.1	100		

Concerning the *second scenario*, the share of energy demand covered by the PV-battery plant is estimated simulating the integrated PV-battery system in a tool implemented in INSEL [50]. More details about the simulations and the results of the PV-battery model are given in the Supplementary Materials. The produced power corresponds to a certain share of the total load, given by the electricity demand of the treatment chain in one year [MWh/y]. The total electricity demand is assumed to be always constant. The remaining demand is supplied by the grid, with the electricity carriers' mix used in the previous scenario (Table 2). In this case, the CO_2 emissions are only due to the fraction of electricity supplied by the grid. Finally, the PV-battery plant located in The Netherlands is compared with an analogous plant located in one of the European regions with the highest solar potential and more precisely in Valencia.

For what concerns the cost of electricity, in the *first scenario* the current cost of electricity for non-household consumers is considered [51]. In the *second scenario* the cost is calculated as the combination of the levelized cost of electricity produced by the PV-battery plant and the cost of electricity from the grid. Regarding the LCOE relevant to the PV-battery plant, the capital costs are calculated as the sum of the cost of the PV modules (specific cost of 1000 €/kW [52]) and of the battery (specific cost of 400 €/kWh plus the cost of the converter, equal to 200 €/kW [53]). The capital costs of the PV panels and the batteries are annualized taking into account a life time of 25 years and a discount rate of 6%. The operating cost of the PV and the battery are calculated as 1.5%/y and 2.5%/y of the investment cost, respectively. Finally, within this scenario, in one case the CO_2 emissions are assumed to be subjected to no

taxation, while in the other case an average CO_2 price of 80 €/ton_{CO2} is also considered for the calculation of the LCOE [59].

3. RESULTS AND DISCUSSION

The wastewater contains sodium and chloride ions, as well as the bi-valent ions, which are removed from the spent resins during the regeneration process. The composition of the real wastewater, produced by the water softening plant in The Netherlands, is reported in Table 3.

Table 3. Composition of the wastewater produced by the water softening process.

C_{Na} [mol/m^3]	C_{Cl} [mol/m^3]	C_{Mg} [mol/m^3]	C_{Ca} [mol/m^3]	C_{SO4} [mol/m^3]
173.9	662.2	55.6	191.7	3.125

Within each treatment chain, the concentration step has to make the concentration of the produced brine equal to the one of the fresh reactant required by the regeneration process. Therefore, for any chain, one of the constraints used for the design of the concentration technologies consists in the concentration of the outlet brine, which has to be equal to 90,000ppm. In the case of the chain with the RO-MD system, the RO retentate concentration is always fixed and equal to the maximum achievable concentration, equal to 70,000ppm [54]. The final concentration increase up to 90,000ppm is covered by the MD unit.

In the following, these processes are compared varying the operating conditions and the energy supply. Table 4 summarizes the scenarios presenting different energy supply systems and, for each scenario, the parametric analyses performed varying technical (Q_{feed}), economic ($Cost_{El}$ and $Cost_{Heat}$) and environmental ($f_{CO2,emission}$) inputs. In the analyses in which the feed flow rate is fixed, the value of 130 m^3/h was chosen in agreement with the volumes of effluent produced in real plants.

Table 4. Summary of the analyses reported in the present work.

	Scenario	Variable input	Fixed inputs
Wastewater: spent IEX regenerant solution	Scenario 1. Electricity supply: grid only (Section 3.1)	Q_{feed} (10-150m^3/h) (Section 3.1.1)	$Cost_{El}$=0.103 \$/kWh Waste heat, $Cost_{Heat}$=0.01\$/kWh
		Q_{feed} and $Cost_{Heat}$ (different heat sources) (Sections 3.1.2)	$Cost_{El}$=0.103 \$/kWh
	Scenario 2. Electricity supply: PV-battery-grid (Section 3.2)	$Cost_{El}$ and $f_{CO2,emission}$ (different PV-battery plant configurations) (Sections 3.2.1 and 3.2.2)	Q_{feed}=130 m^3/h Waste heat, $Cost_{Heat}$=0.01\$/kWh

3.1 Scenario 1. Electricity supply from the grid

In the first scenario the electricity is supposed to be completely supplied from the grid with a fixed cost, which is the current cost of electricity for non-household consumers in The Netherlands, equal to 0.086€/kWh (0.103\$/kWh in 2018).

3.1.1. Feed flow rate variation

Firstly, the three systems are compared varying the feed flow rate of the effluent sent continuously to the treatment chain: the feed flow rate variation gives rise to a variation of the required size of the plant, and, consequently, of the investment cost and to a proportional variation of the operating costs due to the energy consumption. The impact of the feed flow rate on the capital and operating levelized cost is reported in Figure 2.

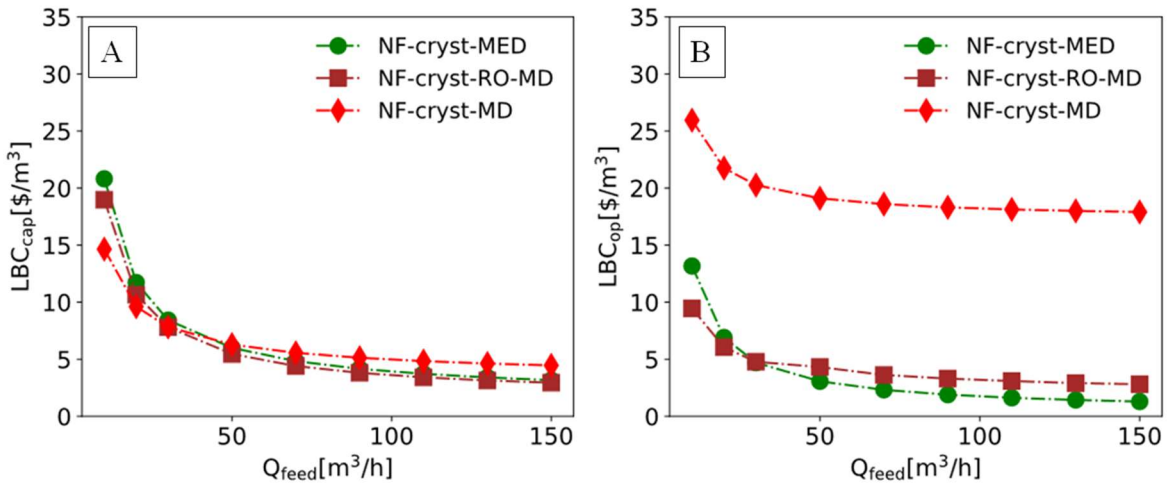

Figure 2. LBC_{cap} (A) and LBC_{op} (B) of the three chains (NF-cryst-MED, NF-cryst-RO-MD, NF-cryst-MD) as a function of Q_{feed} [m^3/h]. Electricity from the grid, $Cost_{El}$=0.103$/kWh; waste heat available in the industrial site, $Cost_{Heat}$=0.01$/kWh.

Figure 2A shows how the LBC_{cap} is influenced by the feed flow rate: according to economy of scale, the highest levelized cost is found at the lowest flow rates, while much lower and slowly decreasing values are observable at high feed flow rates. The three systems exhibit the same trend. However, at very low flow rates the MED-chain has the highest LBC_{cap} because of the higher investment cost associated with the MED plant. Conversely, RO and MD are typically modular technologies and show lower investment costs at low scales. At higher flow rates, the situation changes and the RO-MD chain results as the most convenient system, even if the LBC_{cap} is very close to the one of the MED system. Finally, the LBC_{cap} reached at higher feed flow rates with the MD technology is the highest because of the very high number of modules to be arranged in series and in parallel. The design flow rate of each commercial MD module is fixed and the flow rate defines the required number of branches in parallel in which the feed is distributed. Moreover, since the recovery of the single MD unit is thermodynamically low, it is necessary to arrange more modules in series and in particular, each branch in parallel presents 15 modules in series in the first stage and 8 in the second stage.

Regarding the operating cost, Figure 2B shows the trend of the LBC_{op} varying Q_{feed} for the three systems. At low flow rates, the trends present an evident diminution, due to the variation of the maintenance costs, which depend directly on the investment costs. Conversely, at higher flow rates, the profiles are almost constant, since most of the operating costs are due to the energy demand and these are linearly proportional to the feed flow rate. Notably, the MD-chain operating costs are much higher than the others in the whole range of Q_{feed} because of the very high thermal energy demand of the MD process. The combination of LBC_{cap} and LBC_{op} (which includes the revenues coming from minerals and water production) gives rise to LBC_{tot}, reported in Figure 3.

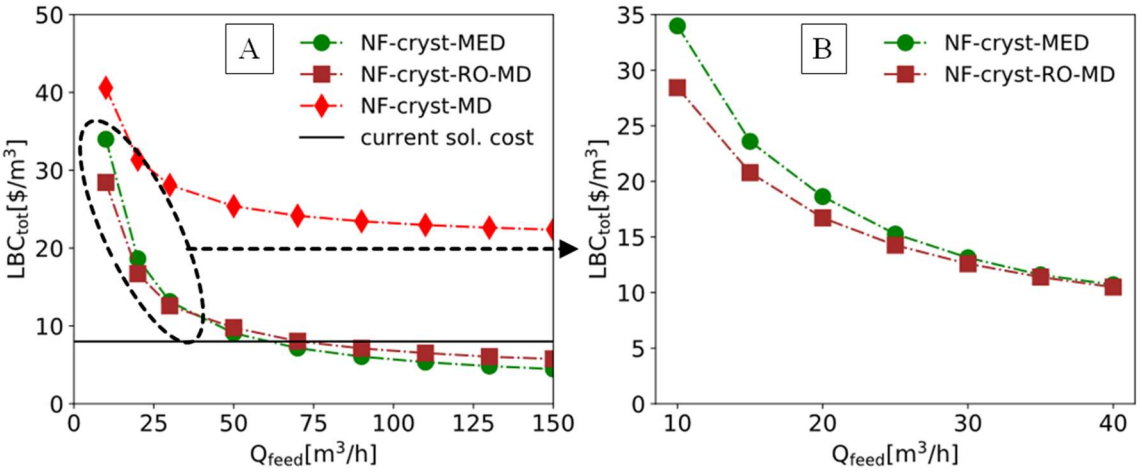

Figure 3. (A) LBC_{tot} of the three chains (NF-cryst-MED, NF-cryst-RO-MD, NF-cryst-MD) as a function of Q_{feed} [m^3/h] and (B) a zoom in the low flow rates region to compare the most performing chains (NF-cryst-MED and NF-cryst-RO-MD). Electricity from the grid, $Cost_{El}$=0.103$/kWh; waste heat available in the industrial site, $Cost_{Heat}$=0.01$/kWh.

The comparison of the LBC_{tot} of the three systems highlights that the chains with MED and with RO-MD behave similarly, while the chain with MD only shows much higher LBC_{tot} values in the whole range of Q_{feed}, because of the crucial operating cost due to the MD thermal demand. Interestingly, the curves of LBC_{tot} of the two most performing systems intersect at a feed flow rate of around 40m^3/h (see the zoom in Figure 3B): at lower flow rates the RO-MD system is more convenient because of its modularity which leads to lower investment costs, while at higher flow rates the MED system is more feasible thanks to the lower global energy requirements. Finally, it is remarkable that in a very wide range of Q_{feed} (higher than 60m^3/h for the MED chain and higher than 70m^3/h for the RO-MD chain) the LBC_{tot} falls below the current cost of the fresh regenerant solution (Figure 3A). This implies that both chains are more convenient from an economic point of view with respect to the state of the art which provides a continuous supply of fresh reactant at a cost of 8$/$m^3$.

For what concerns the energy requirements, the total electricity and heat demand of the three chains varying the feed flow rate are reported in Figure 4.

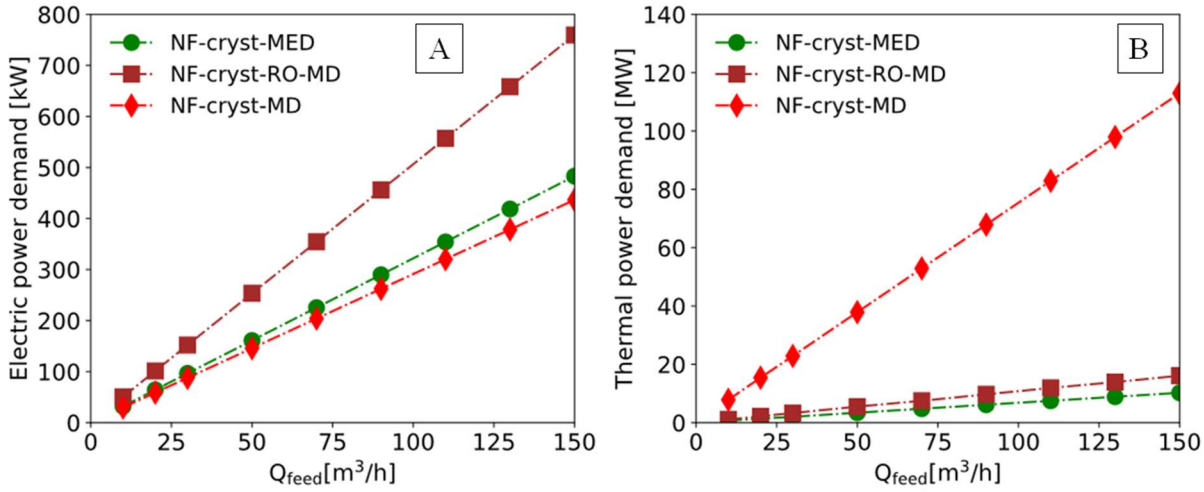

Figure 4. Electric (A) and thermal (B) power demand for the three chains varying the feed flow rate.

Firstly, in all cases, both electricity and heat demand show a linear trend, as expected. The RO-MD chain shows the highest electricity demand, since the RO unit is a pressure-driven process. However, the difference among the electricity demands of the three chains is not as evident as the difference among the thermal energy demands. The MD-chain exhibits a much higher heat demand than the other two. Also, the RO-MD chain presents a thermal energy demand slightly higher than the MED one. The MD process is known to have a greater heat requirement in comparison to the MED: in our simulations, the MD specific energy demand is around 900kWh$_{th}$/m$^3_{dist}$, which is in agreement with the values found by Ali et al. for continuous systems with high recovery, which ranged between 800 and 1200kWh$_{th}$/m$^3_{dist}$ [55]. Therefore, also in the case of the combination with the RO unit, MD leads to an increase of the thermal energy demand of the overall chain beyond that of the MED chain, even if MD is supposed to cover only a small fraction of the concentration change (from the highest concentration achievable in the RO, i.e. 70,000ppm, up to 90,000ppm).

Finally, the environmental impact of the three chains is assessed looking at the CO_2 emissions due to the energy production. Since the thermal energy is supposed to be industrial waste heat, additional electricity is considered for pumping and compressing the heat. The guidelines report a default value of 0.09GJ of electric energy required per GJ of heat recovered [56]. Thus, this electricity demand is also taken into account for the calculation of the CO_2 emissions. Figure 5 shows the CO_2 emissions due to the total energy demand of the three treatment chains.

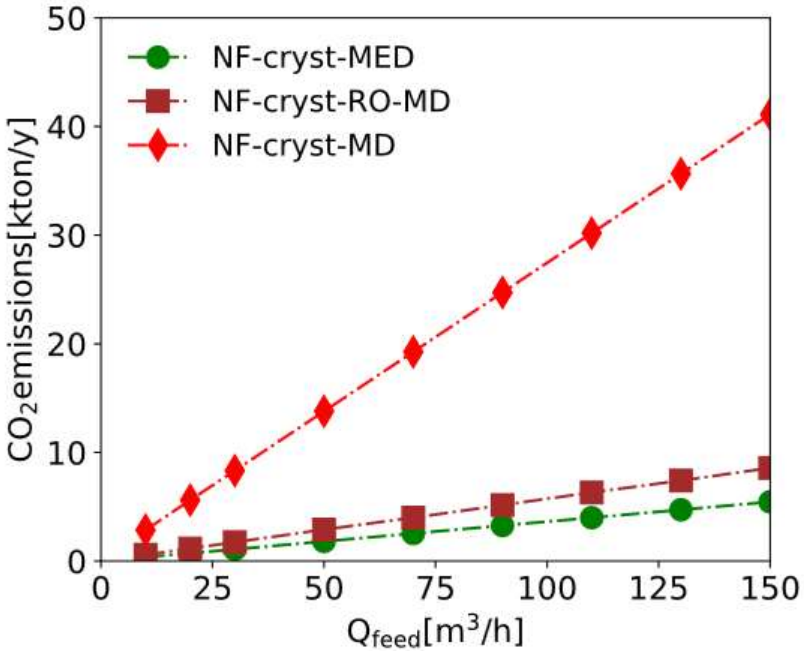

Figure 5. CO_2 emissions of the three treatment chains, considering the current power generation mix from the grid and assuming a demand of $0.09GJ_{el}$ for each GJ of waste heat recovered.

Also from an environmental point of view, the MD chain is the worst performing, because of its large energy demand. Conversely, the other two chains show lower emissions. To compare the environmental impact of the chains with the one of the current industrial process, it has to be considered that currently the salt-water solution is given as a fresh reactant in every regeneration cycle. In the regeneration phase, a water softening plant consumes a large amount of water for the regenerant and the rinse solution: the total effluent flow rate produced is given by the sum of these two solutions which contribute with an approximate ratio of 1:9. Therefore, during the regeneration, assuming a continuous mode, a plant producing around $130m^3/h$ of effluent firstly receives the regenerant solution with a flow rate of $13m^3/h$ and secondly receives pure water, as the rinse solution, with a flow rate of $117m^3/h$. For the preparation of the regenerant solution, around 10,000ton/year of NaCl are required, whose production is very energy intensive: the electricity demand for salt crystallization by mechanical vapour recompression is $450kWh/ton_{salt}$ [57]. The energy demand of the salt production process, taking into account the yearly requirement of salt in the plant, leads to around 2.1kton/y of CO_2 emissions. On top of this, the emissions due to the production of the demineralized water used for the preparation of IEX regenerant solution and the salt transportation should be accounted. However, these terms are too site-specific and, conservatively, have not been considered in this study. For easiness of comparison, we calculated the ratio between the CO_2 emission and the produced regenerant solution, which

results equal to 19.7$kg_{CO2}/m^3_{regenerant}$. In the proposed treatment systems, the MED and the RO-MD chains treat the same flow rate of effluent (130m^3/h) and produce around 53m^3/h of brine solution, reusable as regenerant. The chains show global values of CO_2 emissions equal to 4.7 and 7.3kton/y respectively, which correspond to a ratio between the CO_2 emissions and the produced brine of 10.8 and 16.7$kg_{CO2}/m^3_{regenerant}$. Thus, it is possible to reduce the CO_2 emissions, with both chains, even considering the current energy mix of the grid.

3.1.2 Simultaneous variation of feed flow rate and energy cost

To investigate also the role of the thermal energy cost, a simultaneous variation of feed flow rate and thermal energy cost is performed. Three different heat sources are considered for the definition of the cost: industrial waste heat available in the site, gas turbine co-generation cycle and boiler burning natural gas. The heat costs relevant to the three cases define a range, which covers the costs from 0 up to about 0.07\$/kWh_{th}, in the case of the boiler where natural gas at a cost of 0.065\$/kWh is burnt with an efficiency of 90% [58].

Only the NF-cryst-MED and the NF-cryst-RO-MD chains are analysed, since the NF-cryst-MD chain turned out as the worst performing in all cases. Figure 6 reports the contour-maps of the LBC_{tot} of the two chains varying feed flow rate and heat cost. The line in black collects all the points in which the LBC_{tot} results equal to 8\$/m^3, which is the value used as a threshold, since it is the current cost of the regenerant solution. All cases in the region above the line are feasible, since their LBC_{tot} results lower than 8\$/m^3. In both cases, the feasibility area enlarges when Q_{feed} increases, since the levelized capital costs are lower and a higher expense for the thermal energy can be met within the feasibility region. Comparing the two technologies, the NF-cryst-RO-MD chain shows a smaller feasibility area and this is explicable considering its higher energy requirement. However, the minimum flow rate found in the feasibility region is lower in the case of the NF-cryst-RO-MD chain (around 38m^3/h) and this demonstrates that this system is more economically convenient in the case of lower plant size. Overall, both systems show a significantly wide range of operating conditions where they result more competitive than the state of the art from an economic point of view.

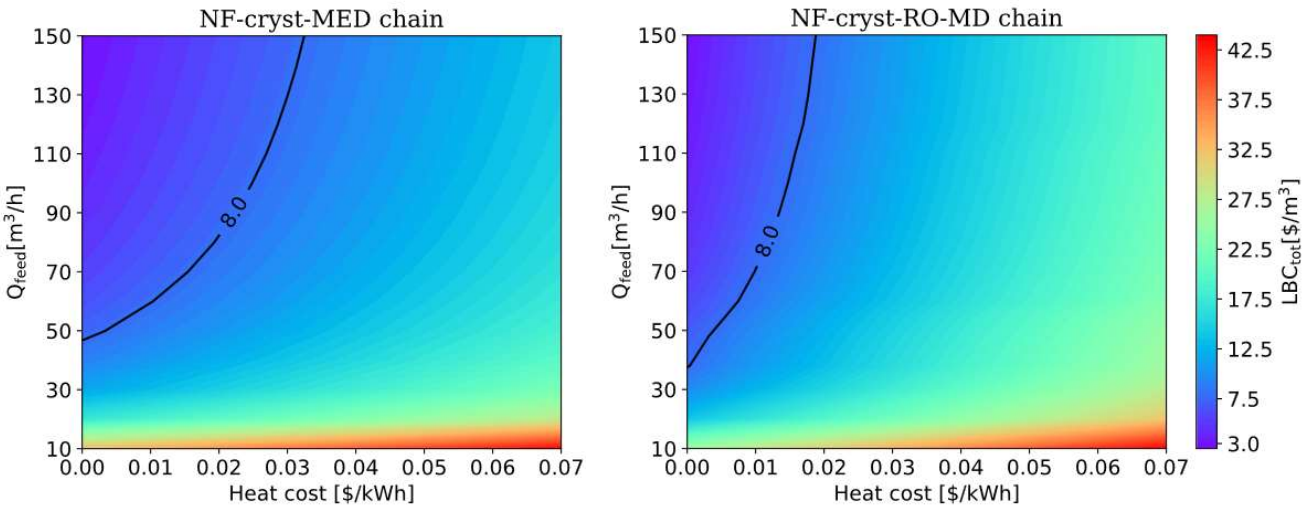

Figure 6. Contour maps of the LBC_{tot} of the NF-cryst-MED chain (left) and of the NF-cryst-RO-MD chain (right) varying Q_{feed}[m^3/h] and $Cost_{Heat}$[$/kWh]. Electricity from the grid, $Cost_{El}$=0.103$/kWh. The black line corresponds to all the cases in which the LBC_{tot} results equal to 8$/$m^3$, which is the current cost of the fresh regenerant solution.

3.2 Scenario 2. Electricity supply from a photovoltaic plant coupled with battery storage

3.2.1 PV-battery plant configurations: global LCOE and emission factors

In the second scenario, the electricity is supplied by a dedicated photovoltaic plant coupled with a standard Li-Ion battery storage. On the basis of the meteorological characteristics of the location, the share of the total demand covered by renewables is derived; the rest is taken from the grid, assuming a fixed purchase price, equal to the one used in Scenario 1. Parametric analyses varying the installed PV power and the capacity of the battery give rise to a scatter of LCOE values as a function of the CO_2 emission factor. The configurations found in correspondence to the lower envelope of the scatter plots, showed in Figure 7, are used for the definition of the LCOE values and the corresponding emission factors in Scenario 2. In chart A, the emissions are supposed to be subjected to no taxation, while in chart B the CO_2 emissions are taxed with a price of 80€/ton. More details about the PV-battery plant simulations and about Figure 7 are given in the Supplementary Materials.

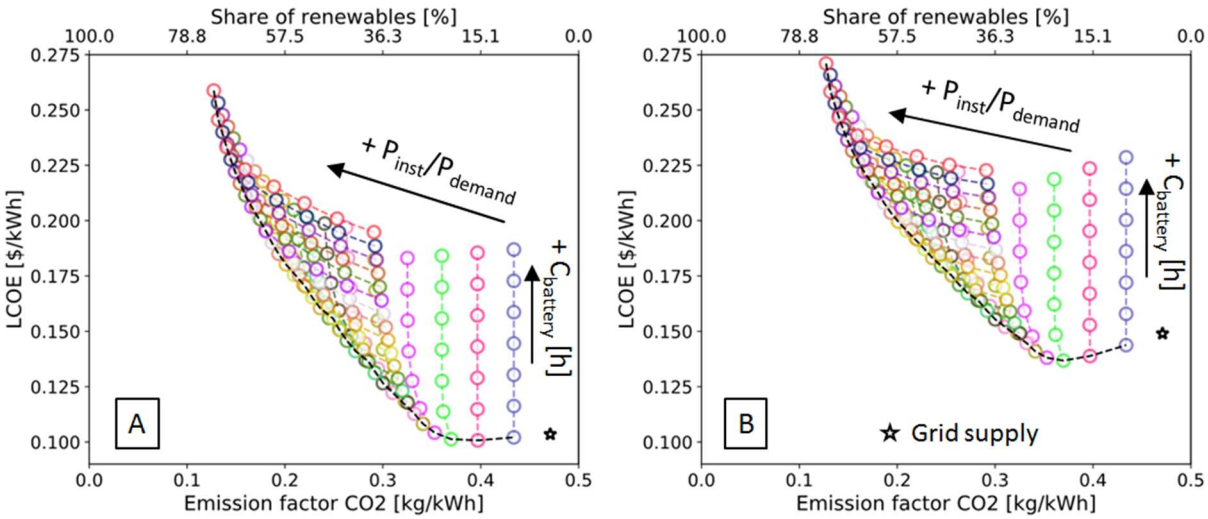

Figure 7. LCOE [$/kWh] of the PV-battery-grid supply as function of the CO_2 emission factor from the grid [kg/kWh] varying the P_{inst}/P_{demand} ratio from 0.5 to 10 and the full load hours of the battery from 0 to 17.5h. Figure A refers to a scenario where the CO_2 emissions are not subjected to taxation, while in Figure B the CO_2 emissions have a cost of 80€/ton_{CO2} [59]. Star symbol indicates the grid supply point.

3.2.2 Treatment chains results

The NF-cryst-MED and NF-cryst-RO-MD chains are compared varying the electricity cost within the range found in Figure 7. Figure 8A shows the trends of LBC_{tot} varying the LCOE within the ranges reported in Figure 7A and B for the two chains, while Figure 8B reports the variation of LBC_{tot} with the specific CO_2 emissions. In the first chart, for each chain, the LBC_{tot} trends with or without the taxation on the CO_2 emissions are partially overlapped, since part of the estimated LCOE range is the same, even if in correspondence to different CO_2 emission factors (see Figure 7A and B). The two chains exhibit a linear trend of LBC_{tot} with the cost of electricity, since the total electricity cost is the only varying term and it linearly depends on the given LCOE. Notably, even if the LCOE becomes more than two times the value of the electricity cost from the grid, the competitiveness of both chains is ensured almost in all cases: the MED chain presents values of LBC_{tot} much lower than the current cost of the regenerant solution in the full range of LCOE, while the RO-MD chain presents values of LBC_{tot} slightly higher than the current cost of the regenerant solution only for LCOE values higher than 0.25$/kWh. Figure 8B shows how much the LBC_{tot} increases when the CO_2 emissions decrease, in correspondence to higher shares of renewables in the energy supply system. As expected, the difference between the cases with or without taxation becomes more evident in the systems with higher shares of electricity from the grid, while at

low CO_2 emissions the differences are negligible. Finally, it is remarkable the difference in the CO_2 emissions between the case in which the electricity is fully supplied by the grid (Scenario 1, represented by the star marker) and the cases analysed in Scenario 2. Therefore, with a PV-battery system, it is possible to reduce dramatically the emissions and, at the same time, ensure the economic feasibility of both chains. In the case with CO_2 taxation, the most environmentally friendly and feasible systems are the MED chain with LBC_{tot} of 6.1\$/m^3_{brine} and CO_2 emissions of 2.9kg_{CO2}/m^3_{brine} and the RO-MD chain with LBC_{tot} of 7.9\$/m^3_{brine} and CO_2 emissions of 5.1kg_{CO2}/m^3_{brine}. Both values result lower than the current CO_2 emissions due to the production of fresh NaCl, equal to 19.7$kg_{CO2}/m^3_{regenerant}$. Therefore, both chains ensure a significant reduction of the CO_2 emissions with respect to the current system, which is around 85% with the MED chain and around 75% for the RO-MD chain.

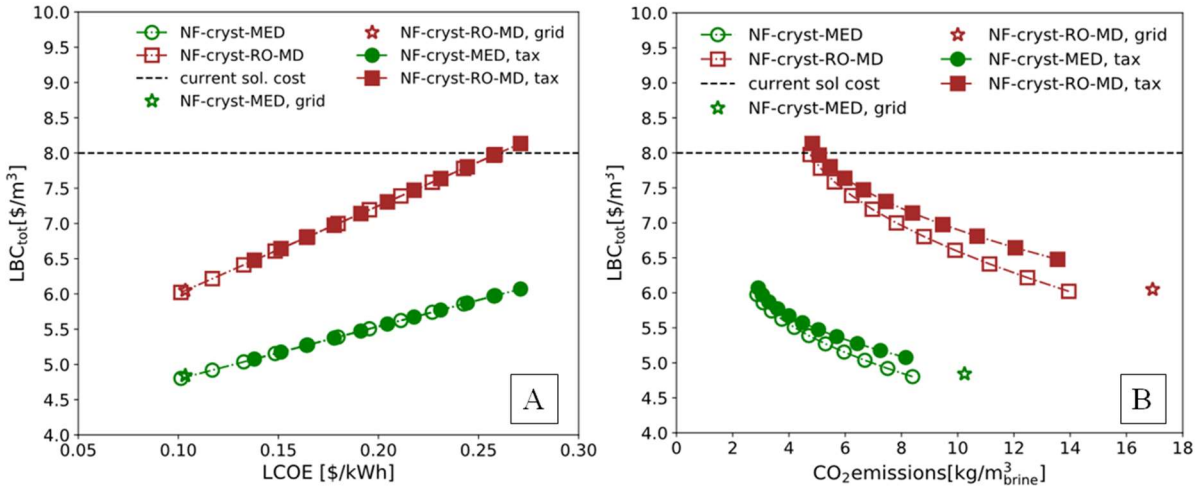

Figure 8. LBC_{tot} vs. LCOE for the NF-cryst-MED and the NF-cryst-RO-MD chains (A) and LBC_{tot} vs. the CO_2 emissions for the two same chains (B), with and without taxation on the CO_2 emissions. The star marker points represent the cases with a full supply from the grid (Scenario 1).

3.2.3 Impact of the meteorological characteristics: comparison with a plant in Valencia, Spain

The analysis discussed above is performed also considering a different location for the plant: Valencia in Spain. The location has been selected since Valencia belongs to one of the European regions with the highest solar potential. For this reason, the share of the energy demand covered by the renewables is much higher than in The Netherlands and the LCOE is consequently lower. Figure 9 shows the lower envelopes of the scatter plot of LCOE vs. CO_2 emission factor for the case of a plant located in Rotterdam (shown in Figure 7) and in Valencia with or without CO_2 taxation. Notably, the difference between the corresponding

curves for Valencia and for Rotterdam increases moving to the region of lower CO_2 emissions. This is because the installed PV power necessary to reach high shares of renewables decreases dramatically for the plant located in Valencia. Therefore, it is evident that the LCOE trend is flatter in this last case, especially in the scenario with the tax on the CO_2 emissions. Finally, in both trends relevant to Valencia, the minimum occurs for configurations with higher shares of renewables with respect to the trends for Rotterdam, because of the lower costs of the PV-battery plants in correspondence to the same share of renewables.

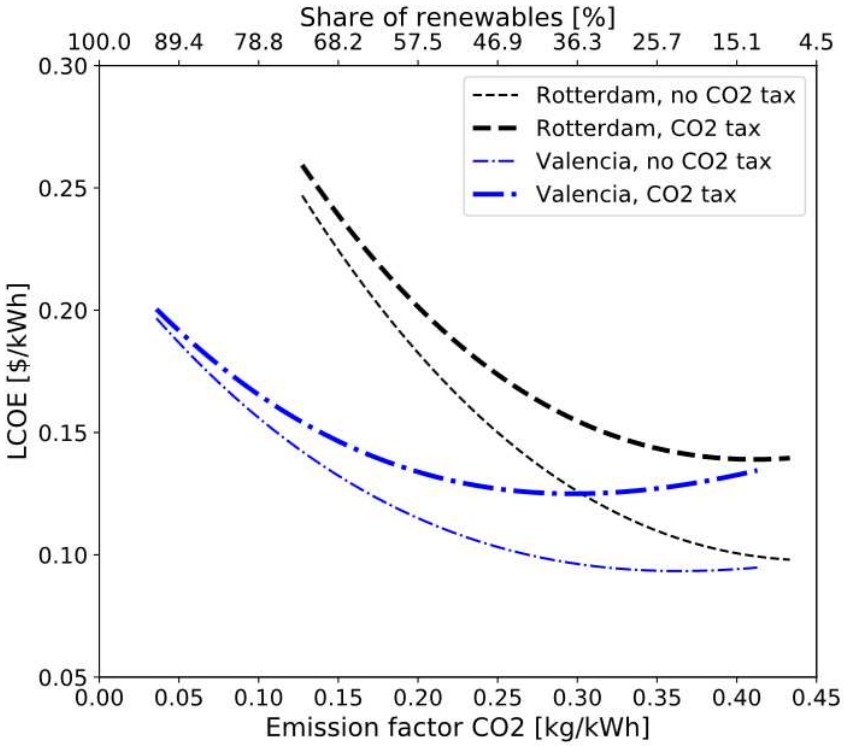

Figure 9. Lower envelopes of the scatter plots of LCOE [$/kWh] vs. the CO_2 emission factor [kg/kWh], varying P_{inst}/P_{demand} between 0.5 and 10 and $C_{battery}$ between 0 and 17.5h, for the case of a plant located in Rotterdam (case study) and in Valencia (Spain). The thinner lines correspond to no taxation on the CO_2 emissions, while the thicker lines to a taxation of 80€/ton_{CO2}.

The LCOE values calculated for the plant in Valencia are employed as inputs for the two selected chains and the resulting LBC_{tot} values are reported vs. the CO_2 emissions and compared with the results for the Rotterdam case in Figure 10. In this analysis, only the LCOE values obtained assuming a fixed taxation on the CO_2 emissions are considered. Both chains show a much flatter trend of LBC_{tot} vs. the specific CO_2 emissions, since the LCOE trend resulted to have slighter variations with the CO_2 emission factor in the case of Valencia. It is remarkable the shift of both LBC_{tot} trends towards lower CO_2 emissions, since the maximum share of energy demand supplied via renewables is 92%, while in the Rotterdam

case the maximum share of renewables was around 73%. Moreover, in this case, both chains result to be economically feasible in the whole range of LCOE, since, even in the case which minimizes the CO_2 emissions, the LBC_{tot} of both chains is lower than the current cost of the regenerant solution. This analysis shows the high potential of the proposed systems, which result economically competitive and able to guarantee a significant reduction of the CO_2 emissions (especially when coupled with a renewable energy supply). In fact, the CO_2 emissions go down to $0.77 kg_{CO2}/m^3_{brine}$ in the case of the MED chain and to $1.26 kg_{CO2}/m^3_{brine}$ in the case of the RO-MD chain. Thus, in both cases, a reduction of the emission of more than 90% compared to the current system is achieved.

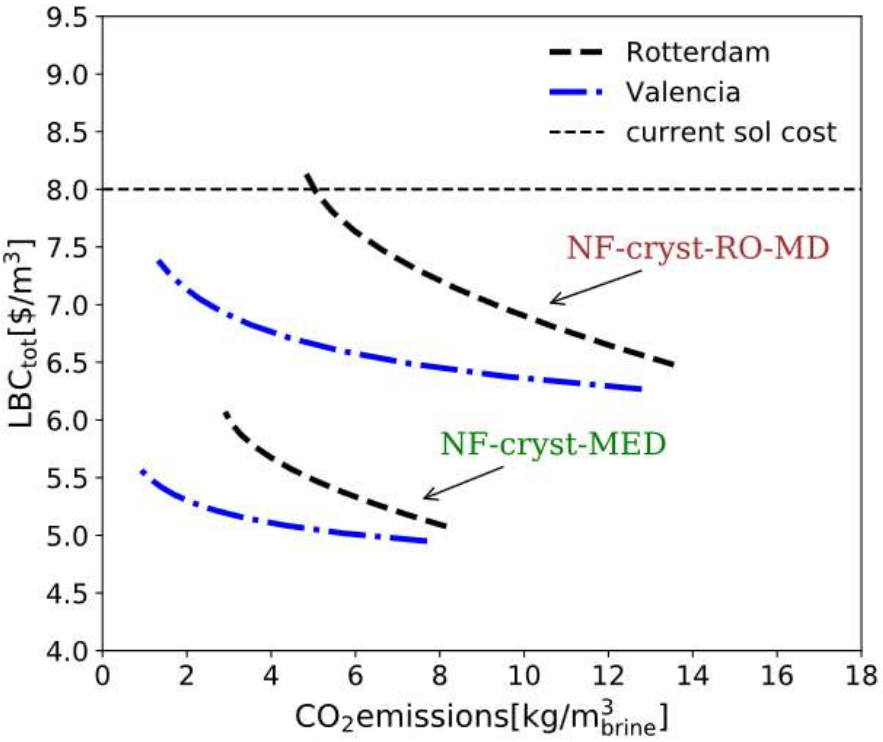

Figure 10. Comparison of the LBC_{tot} trends [$/m$^3_{brine}$] of the two chains (NF-cryst-MED and NF-cryst-RO-MD) vs. the CO_2 emission factor [kg/kWh], assuming CO_2 taxation of 80€/ton$_{CO2}$, for the case of a plant located in Rotterdam (case study, in black) and in Valencia, Spain (in blue).

3.3 Implications

The results of the investigated systems in the different scenarios have been compared looking at the global outputs, to summarize the implications of the proposed strategies in terms of economic feasibility and environmental impact. Figure 11 reports the LBC_{tot} and the CO_2 emissions per m^3 of produced brine (kg_{CO2}/m^3_{brine}). In particular, the current CO_2 emissions due to the fresh NaCl salt production are compared with the ones due to the treatment chains' energy demand (i) when the electricity is fully taken from the grid and (ii) when the electricity

is partially supplied by a PV-battery system, in the two different locations and with the maximum share of renewables at which the LBC_{tot} resulted lower than the threshold value. The corresponding values of LBC_{tot} are also compared with the current cost of the fresh regenerant solution. Notably, all systems ensure a reduction of the CO_2 emissions and a more competitive LBC_{tot} in comparison with the current system. Notably, the employment of renewable energy sources allows a net reduction of the CO_2 emissions, but the LBC_{tot} results higher than in scenario 1; conversely, the relatively low cost of the electricity taken from the grid leads to lower LBC_{tot} but the reduction of CO_2 emissions is less significant than in scenario 2.

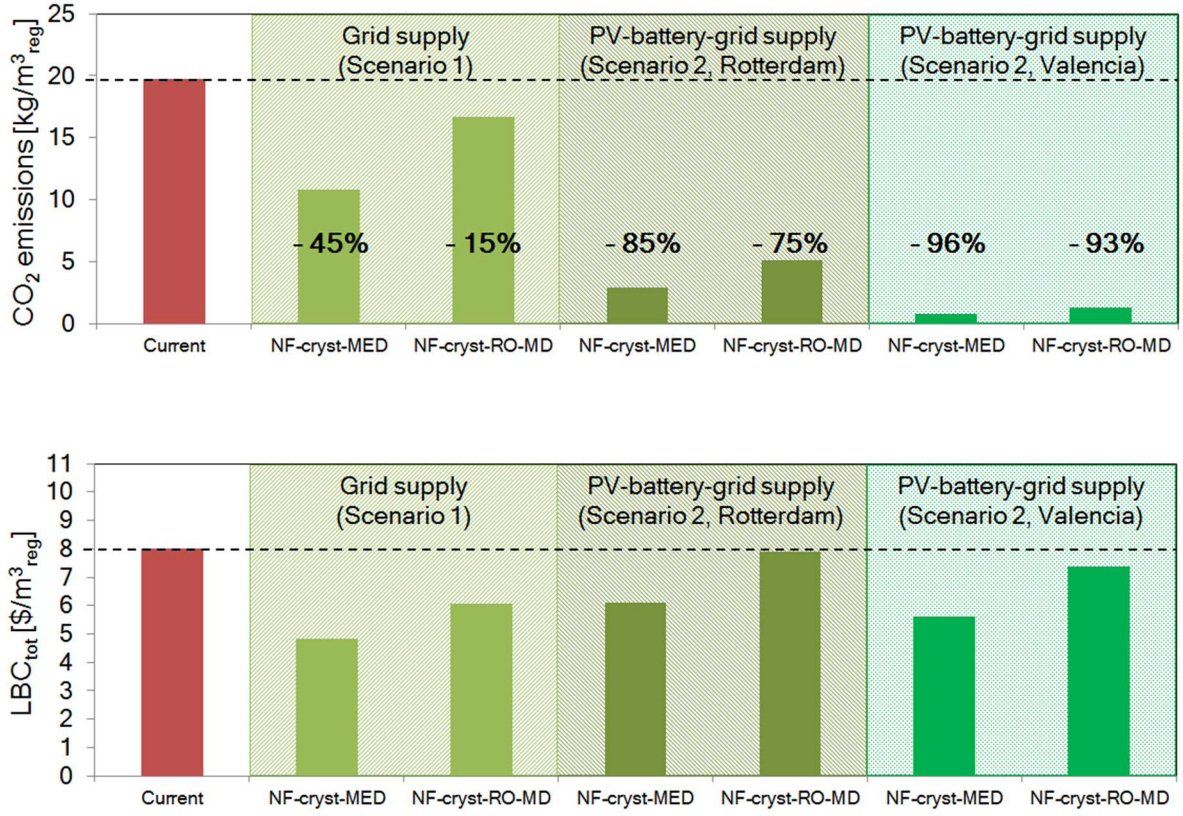

Figure 11. Values of CO_2 emissions divided by the produced regenerant (figure above) and the corresponding LBC_{tot} (figure below) for the current case and for the analysed scenarios. For the scenario 2, the values corresponding to the minimum emissions (maximum share of renewables) were selected. Q_{feed}=130m^3/h; waste heat, $Cost_{heat}$=0.01$/$kWh_{th}$.

4. CONCLUSIONS

This work presents a comprehensive analysis of different strategies to implement a circular economy approach in the water softening industrial sector. These strategies aim (i) at recycling the effluent and reusing it as reactant in the regeneration of the IEX resins and (ii) at

recovering valuable raw materials. For the first time, different concentration technologies and different energy supply systems were proposed in order to identify the most economically convenient and environmentally friendly system to treat the wastewater. With this regard, the impact of different drivers as the employment of self-generated energy and the meteorological characteristics of the location has been investigated. The proposed treatment chains include a pre-treatment step, composed of nanofiltration and crystallization, and a concentration step. Three alternative concentration technologies have been evaluated: MED, MD and the combination of RO and MD. The system composed by nanofiltration, crystallizers and membrane distillation turned out as the worst performing in all cases varying the feed flow rate. Conversely, the system with RO-MD resulted more convenient at lower scales because of the lower investment costs and the chain with the MED resulted to have a lower LBC at higher plant scales, because of the lower energy requirements. Concerning the environmental aspects, the CO_2 emissions per m^3 of regenerant solution found for the MED chain and the RO-MD chain were lower than those due to the production of the NaCl salt, in the case of electricity supplied by the grid. Moreover, the simultaneous variation of feed flow rate and thermal energy cost allowed assessing the set of operating conditions for which the two chains resulted feasible. Overall, the range of feasible heat costs was wider for the MED system, but the RO-MD system resulted feasible in a slightly larger range of feed flow rates.

Furthermore, the impact of supplying self-generated energy to the chains was assessed, by coupling them with a PV-battery plant. With this regard, the trend of LCOE vs. the CO_2 emissions was found varying the installed PV power and the capacity of the battery. Two locations were considered: Rotterdam, which is the location of the case-study water softening plant, and Valencia, since its solar potential is among the highest in Europe. A large decrease of the emissions was found and the systems resulted economically feasible, even if the LCOE was more than two times the electricity cost from the grid. In particular, for the case-study plant, the CO_2 emission per $m^3_{regenerant}$ resulted 75% and 85% lower than the current ones for the RO-MD chain and the MED chain, respectively. For the case of higher solar potential, the reduction was found higher than 90% for both treatment chains. Overall, the MED chain was found to be economically more convenient and to have lower emissions in most cases, because of the lower energy requirements. However, the chain with RO-MD proved to be more feasible at lower scales and, in general, this system should be taken into account for its higher modularity and flexibility.

In conclusion, according to the results collected, both the above treatment chains should be regarded as valuable options towards the implementation of a circular economy approach in the water softening industry.

ACKNOWLEDGEMENTS

This work was funded by the ZERO BRINE project (ZERO BRINE–Industrial Desalination–Resource Recovery–Circular Economy)-Horizon 2020 programme, Project Number: 730390. www.zerobrine.eu.

NOMENCLATURE

NF	Nanofiltration
Cryst	Crystallizer
MED	Multi-effect distillation
RO	Reverse osmosis
MD	Membrane distillation
IEX	Ion Exchange resins
PV	Photovoltaic
RCE	Remote Component Environment
DSPM-DE	Donnan Steric Pore Model with Dielectric Exclusion
CEPCI	Chemical Engineering Plant Cost Index
DCMD	Direct Contact Membrane Distillation
CAPEX	Capital Expenditure
OPEX	Operating Expenditure
LBC	Levelized Brine Cost
LBC_{CAP}	Capital Levelized Brine Cost
LBC_{OP}	Operating Levelized Brine Cost
GHI	Global Horizontal Irradiance
DHI	Diffuse Horizontal Irradiance
LCOE	Levelized Cost of Electricity
Q_{feed}	Feed flow rate [m^3/h]
$Cost_{El}$	Electricity cost [$/kWh]
$Cost_{Heat}$	Thermal energy cost [$/kWh]
$f_{CO2,emission}$	CO_2 emission factor [kg_{CO2}/kWh]
Subscripts	
req	required (for the brine outlet concentration)
prim energy	primary energy

BIBLIOGRAPHY

[1] "World Commission on Environment and Development, The Brundtland report: 'Our common future." 1987.

[2] K. E. Boulding and H. Jarrett, "Essays from the sixth resources for the future forum on environmental quality in a growing economy," Johns Hopkins University Press, Baltimore, 1966, pp. 3–14.

[3] "Ellen MacArthur Foundation, Towards the Circular Economy-Economic and business rationale for an accelerated transition (part 1)." 2013.

[4] P. Ghisellini, C. Cialani, and S. Ulgiati, "A review on circular economy: the expected transition to a balanced interplay of environmental and economic systems," *Journal of Cleaner Production*, vol. 114, pp. 11–32, 2016.

[5] C. Bakker, F. Wang, J. Huisman, and M. den Hollander, "Products that go round: exploring product life extension through design," *Journal of Cleaner Production*, vol. 69, pp. 10–16, 2014.

[6] F. Zhijun and Y. Nailing, "Putting a circular economy into practice in China," *Sustain. Sci.*, vol. 2, pp. 95–101, 2007.

[7] A. Murray, K. Skene, and K. Haynes, "The Circular Economy: An Interdisciplinary Exploration of the Concept and Application in a Global Context," *Journal of Business Ethics*, vol. 140, pp. 369–380, 2017.

[8] M. Geissdoerfer, P. Savaget, N. M. P. Bocken, and E. J. Hultink, "The Circular Economy - A new sustainability paradigm?," *Journal of Cleaner Production*, vol. 143, pp. 757–768, 2017.

[9] J. Fresner, "Cleaner production as a means for effective environmental management," *Journal of Cleaner Production*, vol. 6, pp. 171–179, 1998.

[10] P. Golinska, M. Kosacka, R. Mierzwiak, and K. Werner-Lewandowska, "Grey Decision Making as a tool for the classification of the sustainability level of remanufacturing companies," *Journal of Cleaner Production*, vol. 105, pp. 28–40, 2015.

[11] L. Janeiro and M. K. Patel, "Choosing sustainable technologies. Implications of the underlying sustainability paradigm in the decision-making process," *Journal of Cleaner Production*, vol. 105, pp. 438–446, 2015.

[12] N. Mirabella, V. Castellani, and S. Sala, "Current options for the valorization of food manufacturing waste: a review," *Journal of Cleaner Production*, vol. 65, pp. 28–41, 2014.

[13] A. Cardinali, S. Pati, F. Minervini, I. D'Antuono, V. Linsalata, and V. Lattanzio, "Verbascoside, Isoverbascoside, and Their Derivatives Recovered from Olive Mill Wastewater as Possible Food Antioxidants," *Journal of Agricaltural and Food Chemistry*, vol. 60, pp. 1822–1829, 2012.

[14] S. Abdelkader, F. Gross, D. Winter, J. Went, J. Koschikowski, S. U. Geissen, and L. Bousselmi, "Application of direct contact membrane distillation for saline dairy effluent treatment: performance and fouling analysis," *Environmental Science and Pollution Research*, vol. 26, pp. 18979–18992, 2019.

[15] A. Gopinath, A. Bahurudeen, S. Appari, and P. Nanthagolapan, "A circular framework for the valorisation of sugar industry wastes: Review on the industrial symbiosis between sugar, construction and energy industries," *Journal of Cleaner Production*, vol. 203, pp. 89–108, 2018.

[16] C. A. Cardona, J. A. Quintero, and I. C. Paz, "Production of bioethanol from sugarcane bagasse: Status and perspectives," *Bioresource Technology*, vol. 101, pp. 4754–4766, 2010.

[17] C. R. Holkar, A. J. Jadhav, D. V. Pinjari, N. M. Mahamuni, and A. B. Pandit, "A critical review on textile wastewater treatments: Possible approaches," *Journal of Environmental Management*, vol. 182, pp. 351–366, 2016.

[18] K. Sarayu and S. Sandhya, "Current Technologies for Biological Treatment of Textile Wastewater–A Review," *Applied Biochemistry and Biotechnology*, vol. 167, pp. 654–661, 2012.

[19] L. Bilińska, M. Gmurek, and S. Ledakowicz, "Textile wastewater treatment by AOPs for brine reuse," *Process Safety and Environmental Protection*, vol. 109, pp. 420–428, 2017.

[20] Y. Man, W. Shen, X. Chen, Z. Long, and M. Pons, "Modeling and simulation of the industrial sequencing batch reactor wastewater treatment process for cleaner production in pulp and paper mills," *Journal of Cleaner Production*, vol. 167, pp. 643–652, 2017.
[21] M. Giagnorio, A. Amelio, H. Gruttner, and A. Tiraferri, "Environmental impacts of detergents and benefits of their recovery in the laundering industry," *Journal of Cleaner Production*, vol. 154, pp. 593–601, 2017.
[22] M. Turek, P. Dydo, and A. Surma, "Zero discharge utilization of saline waters from 'Wesola' coal-mine," *Desalination*, vol. 185, pp. 275–280, 2005.
[23] J. Lopez, M. Reig, O. Gibert, and J. L. Cortina, "Integration of nanofiltration membranes in recovery options of rare earth elements from acidic mine waters," *Journal of Cleaner Production*, vol. 210, pp. 1249–1260, 2019.
[24] D. L. Oatley, L. Llenas, R. Pérez, P. M. Williams, X. Martínez-Lladó, and M. Rovira, "Review of the dielectric properties of nanofiltration membranes and verification of the single oriented layer approximation," *Advances in Colloid and Interface Science*, vol. 173, pp. 1–11, 2012.
[25] V. Geraldes and A. M. B. Alves, "Computer program for simulation of mass transport in nanofiltration membranes," *Journal of Membrane Science*, vol. 321, no. 2, pp. 172–182, 2008.
[26] O. Labban, C. Liu, T. H. Chong, and J. H. Lienhard V, "Fundamentals of low-pressure nanofiltration: Membrane characterization, modeling and understanding of the multi-ionic interactions in water softening," *Journal of Membrane Science*, vol. 521, pp. 18–32, 2017.
[27] Y. Roy, M. H. Sharqawy, and J. H. Lienhard, "Modeling of flat-sheet and spiral-wound nanofiltration configurations and its application in seawater nanofiltration," *Journal of Membrane Science*, vol. 493, pp. 360–372, 2015.
[28] M. Micari, M. Moser, A. Cipollina, M. Bevacqua, A. Tamburini, B. Fuchs, and G. Micale, "Combined Membrane and Thermal Desalination Processes for the Treatment of Ion Exchange Resins Spent Brine," in *13th Conference on Sustainable Development of Energy, Water and Environmental systems*, 2018.
[29] D. Zhou, L. Zhu, Y. Fu, M. Zhu, and L. Xue, "Development of lower cost seawater desalination processes using nanofiltration technologies — A review," *Desalination*, vol. 376, pp. 109–116, 2015.
[30] A. Cipollina, M. Bevacqua, P. Dolcimascolo, A. Tamburini, A. Brucato, H. Glade, L. Buether, and G. Micale, "Reactive crystallisation process for magnesium recovery from concentrated brines," *Desalination and Water Treatment*, pp. 1–12, 2014.
[31] R. Turton, R. C. Bailie, W. B. Whiting, J. A. Shaeiwitz, and D. Bhattacharyya, *Analysis, Synthesis and Design of Chemical Processes*. Prentice Hall, 2012.
[32] R. K. Kamali, A. Abbassi, S. A. Sadough Vanini, and M. S. Avval, "Thermodynamic design and parametric study of MED-TVC," *Desalination*, vol. 222, pp. 596–604, 2008.
[33] H. El-Dessouky, I. Alatiqi, S. Bingulac, and H. Ettouney, "Steady-State Analysis of the Multiple Effect Evaporation Desalination Process," *Chem. Eng. Technol.*, vol. 21, no. 5, pp. 437–451, 1998.
[34] B. Ortega-Delgado, L. Garcia-Rodriguez, and D. C. Alarcon-Padilla, "Opportunities of improvement of the MED seawater desalination process by pretreatments allowing high-temperature operation," *Desalination and Water Treatment,*, vol. 97, pp. 94–108, 2017.
[35] J. Gebel and S. Yüce, *An Engineer's Guide to Desalination.* VBG PowerTech, 2008.
[36] *Filmtec Reverse Osmosis Membranes Technical Manual*. .
[37] M. Wilf, *The Guidebook to Membrane Desalination Technology*. Balaban Desalination Publications, 2007.
[38] A. Malek, M. N. . Hawlader, and J. C. Ho, "Design and Economics of RO seawater desalination," *Desalination*, vol. 105, pp. 245–261, 1996.
[39] D. Winter, J. Koschikowski, F. Gross, D. Maucher, D. Düver, M. Jositz, T. Mann, and A. Hagedorn, "Comparative analysis of full-scale membrane distillation contactors -methods and modules," *Journal of Membrane Science*, vol. 524, pp. 758–771, 2017.
[40] M. Papapetrou, G. Micale, G. Zaragoza, and G. Kosmadakis, "Assessment of methodologies and data used to calculate desalination costs," *Desalination*, vol. 419, pp. 8–19, 2017.
[41] I. Hitsov, K. De Sitter, C. Dotremont, and I. Nopens, "Economic modelling and model-based process optimization of membrane distillation," *Desalination*, vol. 436, pp. 125–143, 2018.

[42] F. Vince, F. Marechal, E. Aoustin, and P. Breant, “Multi-objective optimization of RO desalination plants,” *Desalination*, vol. 222, pp. 96–118, 2008.
[43] S. Al-Obaidani, E. Curcio, F. Macedonio, G. Di Profio, H. Al-Hinai, and E. Drioli, “Potential of membrane distillation in seawater desalination: Thermal efficiency, sensitivity study and cost estimation,” *Journal of Membrane Science*, vol. 323, pp. 85–98, 2008.
[44] B. Van der Bruggen, K. Everaert, D. Wilms, and C. Vandecasteele, “Application of nanofiltration for removal of pesticides, nitrate and hardness from ground water: rejection properties and economic evaluation,” *Journal of Membrane Science*, vol. 193, no. 2, pp. 239–248, 2001.
[45] “Mineral Commodity Summaries,” U.S. Geological Survey, 2017.
[46] T. Mezher, H. Fath, Z. Abbas, and A. Khaled, “Techno-economic assessment and environmental impacts of desalination technologies,” *Desalination*, vol. 266, pp. 263–273, 2011.
[47] M. Micari, M. Moser, A. Cipollina, B. Fuchs, B. Ortega-Delgado, A. Tamburini, and G. Micale, “Techno-economic Assessment of Multi-Effect Distillation process for the Treatment and Recycling of Ion Exchange Resin Spent Brines,” *Desalination*, vol. 456, pp. 38–52, 2019.
[48] IEA, *World Energy Balances 2018*. OECD Publishing, 2018.
[49] “2006 IPCC Guidelines for National Greenhouse Gas Inventories,” .
[50] M. Moser, F. Trieb, and J. Kern, “Development of a flexible tool for the integrated techno-economic assessment of renewable desalination plants,” *Desalination and Water Treatment*, vol. 76, p. 5, 2017.
[51] Eurostat, “Electricity prices for non-household consumers - bi-annual data (from 2007 onwards).” .
[52] J. N. Mayer, “Current and Future Cost of Photovoltaics. Long-term Scenarios for Market Development, System Prices and LCOE of Utility-Scale PV Systems,” Fraunhofer ISE (Study on behalf of Agora Energiewende), 2015.
[53] C. Breyer, S. Afanasyeva, D. Brakemeier, M. Engelhard, S. Giuliano, M. Puppe, H. Schenk, T. Hirsch, and M. Moser, “Assessment of mid-term growth assumptions and learning rates for comparative studies of CSP and hybrid PV-battery power plants,” *AIP Conference Proceedings*, vol. 1850, no. 1, p. 160001, 2017.
[54] U. K. Kesieme, N. Milne, H. Aral, C. Y. Cheng, and M. Duke, “Economic analysis of desalination technologies in the context of carbon pricing, and opportunities for membrane distillation,” *Desalination*, vol. 323, pp. 66–74, 2013.
[55] A. Ali, J. H. Tsai, K. L. Tung, E. Drioli, and F. Macedonio, “Designing and optimization of continous direct contact membrane distillation process,” *Desalination*, vol. 426, pp. 97–107, 2018.
[56] M. Harmelink and L. Bosselaar, “Allocating CO2 emissions to heat and electricity,” Harmelink consulting, 2013.
[57] V. M. Sedivy, “Environmental balance of salt production speaks in favour of solar saltworks,” *Proceedings of 1st International Conference on the Ecological Importance of Solar Saltworks, Santorini*, 2006.
[58] EIA, “Monthly Report of Natural Gas Purchases and Deliveries to Consumers,” 2019.
[59] IEA, *World Energy Outlook 2018*. 2018.